Paper 52-2 has been designated as a Distinguished Student Paper at Display Week 2025. The full-length version of this paper appears in a Special Section of the *Journal of the Society for Information Display (JSID)* devoted to Display Week 2025 Distinguished Papers. This Special Section will be freely accessible until December 31, 2025 via:

https://sid.onlinelibrary.wiley.com/doi/full/10.1002/jsid.2078

Authors that wish to refer to this work are advised to cite the full-length version by referring to its DOI:

https://doi.org/10.1002/jsid.2078

Self-Interference Incoherent Digital Holography Enhanced by Quarter Waveplate Condition Geometric Phase Lens and Cholesteric Liquid Crystal Circular Polarizing Filter for Full Color Imaging

Jin-Hyeok Seo[1], Jae-Won Lee[1], Jung-Yeop Shin[1], Min-Seok Kim[1], Young-Min Cho[1],
Hyeon-Su Jeong[1], Kihong Cho[2], Keehoon Hong[2], and Hak-Rin Kim[1,3]*
[1]School of Electronic and Electrical Engineering, Kyungpook National University, Daegu 41566, Korea
[2]Digital Holography Research Section, Electronics and Telecommunications Research Institute, Daejeon 34129, Korea
[3]School of Electronics Engineering, Kyungpook National University, Daegu 41566, Korea

Abstract

We present quarter waveplate condition geometric phase lens (QW-GPL) based self-interference incoherent digital holography (SIDH) system that can overcome fundamental limitations of conventional GPL based SIDH, induced in R/G/B full color DH acquisition due to chromatic dispersion. Reconstructed DH images can be further improved by adopting cholesteric liquid crystals for circularly polarized light filters at wide ranges of incident angles and wavelengths.

Author Keywords

self-interference incoherent digital holography; geometric phase lens; quarter waveplate; cholesteric liquid crystal.

1. Introduction

In recent years, incoherent digital holography (IDH) has emerged as a transformative phase-imaging technique, extending the applicability of holography beyond the limitations of laser-based coherent imaging systems, which ca provide a way for utilizing incoherent light sources, such as light emitting diode and sunlight. This paradigm shift opens new avenues for 3D holographic imaging in diverse environments, enabling practical applications in medical imaging, security, and augmented reality.

IDH performs 3D wavefront reconstruction using incoherent light sources, overcoming the challenges associated with traditional holography that relies on coherent laser systems. Among IDH techniques, Fresnel incoherent correlation holography (FINCH) is well-known for its ability to capture promisingly full-color holograms, and the one-line FINCH system is called self-interference incoherent digital holography (SIDH). The phase-only spatial light modulator (SLM) is often used in this system as phase shifter. However, conventional SIDH systems face limitations related to the pixel pitch, bulkiness, and calibration issues of SLM [1].

To overcome these limitations, the introduction of conventional half-wave plate condition geometric phase lens (HW-GPL) configuration into SIDH systems has gained much attention. The HW-GPL is ultra-thin LC-based flat lens that operates as a convex lens for right-handed circularly polarized light (RCP) and as a concave lens for left-handed circularly polarized (LCP) light. When the incident light is linearly polarized or unpolarized, the HW-GPL divides the light evenly into convex and concave modes, enabling simultaneous operation in both modes for circular-polarization-based self-interference effects. This HW-GPL was introduced as a replacement for traditional phase modulators [2], such as SLM in FINCH systems, demonstrating superior form-factor properties in its optical module construction [3,4].

In this study, we proposed the integration of a quarter waveplate condition GPL (QW-GPL) configuration into SIDH systems. Conventional HW-GPL-based SIDH systems suffer from unavoidable noise issues due to three-wavefront interference effects in the wide ranges of visible spectrum, caused by the chromatic dispersion outside at the wavelengths from the designed HWP retardation condition. However, the QW-GPL-based SIDH system overcomes these fundamental limitations by providing only two-wavefront modulations for self-interference patterns over whole visible spectrum without the dispersion issues. In our work, the incidence polarization state onto the QW-GPL is controlled by a cholesteric liquid crystal (CLC) for ideal circular polarization for a wide range of incident angle and wavelengths, which also substantially contributes noise-free full-color SIDH imaging.

2. Working principle and experiment results

2.1. QW-GPL based SIDH system

The conventional HW-GPL achieves 100% diffraction efficiency for incident light with RCP or LCP, when the absolute retardation of the birefringent material layer perfectly satisfies the HWP condition. However, if the retardation of the fabricated HW-GPL deviates from the HWP condition, the diffraction efficiency is degraded by the presence of 0^{th} order diffraction (DC term) in addition to reduction on the 1^{st} order diffraction. After passing through a GPL with arbitrary incident polarized light, the polarization state and efficiency term can be described by equations (1) to (4) as follows. $\boldsymbol{\chi_{\pm}}$ represents the polarization state of the transmitted light (RCP: +, LCP: -), and $\boldsymbol{\eta_0}$ denotes the 0^{th} order diffraction efficiency. $\boldsymbol{\delta_{in}}$ indicates the phase profile of the incident beam, while $\emptyset$ refers to the optical axis distribution of the birefringent material recorded in the GPL. As seen in equation (2), the light passing through the GPL acquires a spatially additional phase modulation of $2\emptyset$. As shown in equation (2) to (3), to achieve an ideally functioning GPL that operates as a concave or convex lens with maximum efficiency, the retardation of the fabricated optically anisotropic material layer must satisfy the HWP condition ($\boldsymbol{\Gamma} = \pi$). In this context, $\pm\boldsymbol{S_3}$ denotes the components of the Stokes vector of the incident beam, where +1 corresponds to the RCP state and -1 corresponds to the LCP state. Similarly, if the anisotropic material layer satisfied QWP condition ($\boldsymbol{\Gamma} = \pi/2$) is satisfied, then the 0^{th} order and 1^{st} order diffraction efficiencies will be exactly 50%.

However, as shown in equation (4), the $\boldsymbol{\Gamma}$ is wavelength ($\boldsymbol{\lambda}$) dependent, which implies that 0th order diffraction efficiency may occur for wavelengths other than those for which the GPL is designed as the HWP retardation. Thus, for the conventional HW-GPL scheme, when a linearly polarized light at the designed wavelength is incident, only the $+1^{\text{st}}$ order and -1^{st} order diffractive beams are output, which can provide two-wavefront interference patterns, which does not cause any issue with the

ISSN 0097-996X/25/5602-0700-$1.00 © 2025

acquisition of complex holographic images, as shown in Fig 1(a). However, when linearly polarized (LP) light at wavelengths other than the designed wavelength is incident on the HW-GPL, the additional third wavefront beam of 0th order non-modulated light is induced, leading to three-wavefront interference with generating phase noises during self-interference.

On the contrary, when circularly polarized light is incident on the QW-GPL, two-wavefront-based polarization interference is always maintained even with wavelengths other than the designed wavelength for the QWP retardation, as shown in Fig 1(b). More importantly, at the deviated wavelength conditions from the designed QWP, the relative intensity ratio of 0th order and -1st order diffracted light can be certainly changed from the ideal condition of 1:1, but the phase noise effects can be ideally removed during the phase construction steps in the QWP-based SIDH scheme, differently with the conventional the HWP-based SIDH scheme.

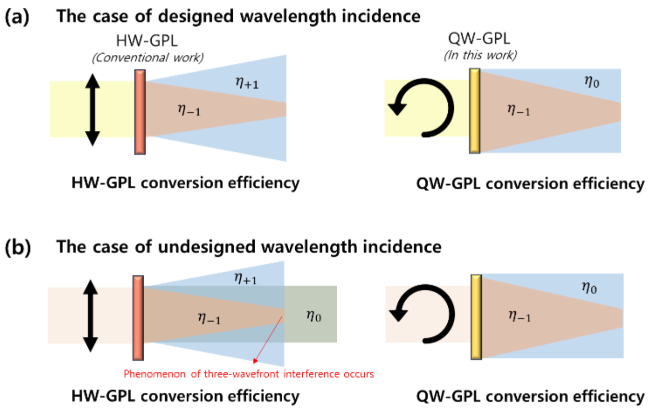

Fig 1. Operation scheme of the wavefront modulation sets for polarization-based self-interference patterns for GPL SIDH systems, when (a) the designed wavelength or (b) the undesigned wavelength is incident on the HW-GPL and QW-GPL.

$$e^{i\delta_{in}}|\chi_{in}\rangle^{GP} \rightarrow \sqrt{\eta_+}e^{i(\delta_{in}+2\Phi)}|\chi_+\rangle + \sqrt{\eta_-}e^{i(\delta_{in}-2\Phi)}|\chi_-\rangle + \sqrt{\eta_0}e^{i\delta_{in}}|\chi_{in}\rangle \qquad (1)$$

$$\eta_0 = \cos^2(\frac{\Gamma}{2}) \qquad (2)$$

$$\eta_{\pm 1} = \frac{1}{2}[1 \mp S_3]\sin^2(\frac{\Gamma}{2}) \qquad (3)$$

$$\Gamma = \frac{2 * \pi * \Delta n * d}{\lambda} \qquad (4)$$

Fig 2(a) is the experimental setup of the conventional HW-GPL-based SIDH system and the proposed QW-GPL-based SIDH system. For the HW-GPL-based SIDH, a linear polarizer is required to direct linearly polarized light into the HW-GPL, and a polarized image sensor is needed to acquire phase shifting digital holographic information after the self-interference patterns modulated from the HW-GPL [5]. And, for the QW-GPL-based SIDH, an achromatic QWP is additionally required to input circularly polarized light into the QW-GPL. A polarized image sensor (polcam, Phoenix 5.0 MP polarization) is an imaging device that four-directional polarization square filter array is overlaid directly on top of the pixel array. This filter consists of repeated 2x2 patterns consisting of grid polarizer with four different angles at 0°,45°,90° and 135°. Thus, it can capture images for a four-phase shifting hologram in a single shot, enabling real-time DH acquisition.

For the comparison and analysis of full-color complex hologram data acquisitions between the HW-GPL-based and the QW-GPL-based SIDH systems, phase-shifting hologram reconstruction steps were performed with 3D full-colored real objects. The reconstructed images from the HW-GPL-based SIDH system showed noise artifacts, such as salt-and-pepper noise, whereas those from the proposed QW-GPL-based SIDH system demonstrated much-reduced noise levels, enabling a higher-quality of full-color DH image reconstruction, as shown in Fig. 2.

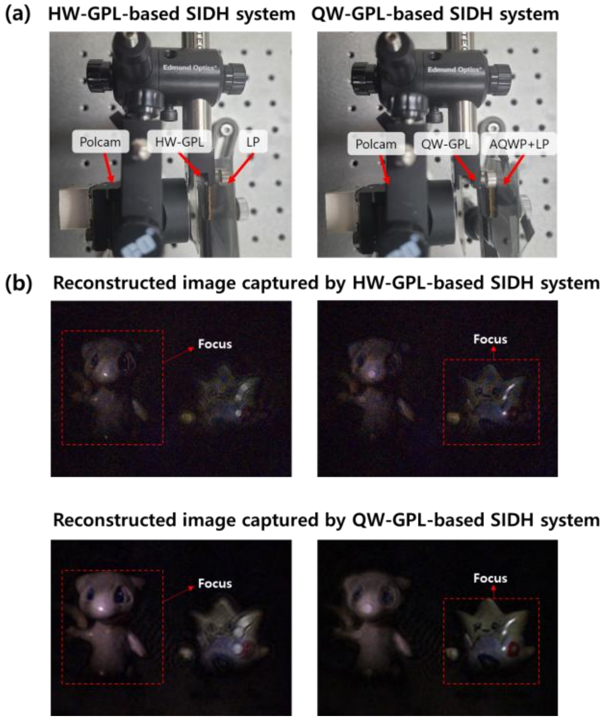

Fig 2. (a) Experimental set-ups for the HW- and QW-GPL-based SIDH systems. (b) Reconstructed full-color images from the HW-GPL SIDH system and the QW-GPL SIDH system.

2.2. QW-GPL based SIDH system with a CLC circular polarizing filter

In Sec. 2.1, for the proposed QW-GPL-based SIDH system, we assumed an ideal circular polarization state as an input beam incident on the QW-GPL. However, conventional achromatic quarter wave plate (AQWP) cannot produce perfectly circularly polarized light across the entire wavelength rage, and the amount of retardation varies with the angle of incidence, making it impossible to direct perfectly circularly polarized light into the QW-GPL, as shown Fig 3(a). Distorted circularly polarized light can be assumed as a combination of left-handed circularly polarized and right-handed circularly polarized light in appropriate proportions. As described in equations (1) to (4), this generates a total of three wavefronts, leading to three-wavefront interference and the introduction of noise. Therefore, this study proposes introducing a CLC polarizing filter into the SIDH system. Unlike conventional QWPs that generate circularly polarized light by controlling retardation through birefringent materials, CLC filters selectively reflect circularly polarized light utilizing its helical chiral structure. This enables the generation of perfectly circularly polarized light within the designed wavelength range, even when light is obliquely incident at angles between about -30° and 30° [6], as shown Fig 3(b).

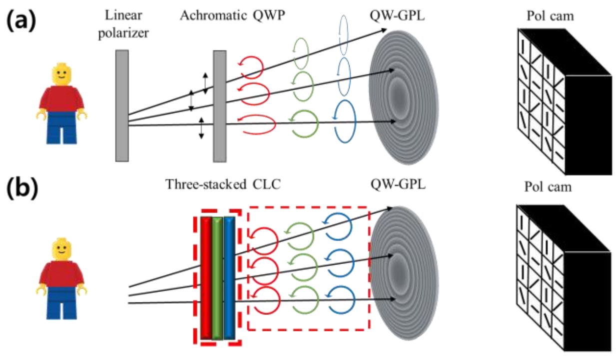

Fig 3. Operation schemes showing polarization conversion states depending on the incident wavelengths and angles, according to the employed GPL conditions: (a) QWP-based achromatic circular polarizer and (b) CLC-based circular polarizer.

The wavelength range for circularly polarized light filtering ($\Delta\boldsymbol{\lambda}$) follows the equation $\Delta\boldsymbol{\lambda} = \boldsymbol{p} \cdot \Delta\boldsymbol{n}$, where $\boldsymbol{p}$ represents the pitch of the birefringent material with chiral properties, and $\Delta\boldsymbol{n}$ means the birefringence value. The pitch is determined by $\boldsymbol{p} = \frac{\boldsymbol{\lambda_C}}{\boldsymbol{n_{avg}}}$,where $\boldsymbol{\lambda_C}$ represents the central wavelength of the CLC polarizer filter operating bandwidth, and $\boldsymbol{n_{avg}}$ means the average refractive index of the birefringent material. In this study, the birefringent material used was E7, with an n_{avg} of 1.639. Consequently, the bandwidth of the CLC cell fabricated with E7 was designed to be 50~60 nm in the visible spectrum. Since a single CLC cell cannot cover the full-color spectrum, the bandwidth center wavelengths of the CLC cells were aligned with the central wavelengths of the polarization camera's color filters: red (620 nm), green (540 nm), and blue (450 nm). Three CLC cells corresponding to red, green, and blue were fabricated and used as circularly polarized light filters. In the future, three CLC stack module can be made into a single cell by adopting a CLC cell with a gradient pitch condition.

Fig 4(a) visually confirmed the color-selective reflection properties of each CLC cells and their three-stacked results. Additionally, the spectral evaluations on the CLC cells are shown in Fig 4(b), for their $\Delta\boldsymbol{\lambda}$ and $\boldsymbol{\lambda_C}$ chracterizations. When we design the circularly polarized reflective and transmissive spectrum of each CLC cell for the three-stacking module, we considered the color filter bandwidths of the employed polcam used for DH acquisitions, to match each other in their spectral properties, as shown in Fig. 4(b).

Fig 5 shows the experimental QW-GPL-based SIDH setup employed with the conventional circular polarizer (LP + AQWP) and with the proposed the three-stacked CLC module. With a full-colored 3D real object, we compared the phase-reconstructed complex DH results between two schemes, as shown in Fig. 6. Here, the image entropy analysis method was used for the quantitative evaluation on noise levels between two QW-GPL-based SIDH systems. The image entropy analysis method is a statistical approach that quantitatively measures the randomness or irregularity in the pixel intensity distribution of an image. It is primarily used to evaluate image quality during the denoising process. If the entropy decreases after noise removal, it indicates that the noise has been effectively removed while preserving important details [7]. Fig 6 presents the reconstructed results obtained after acquiring complex hologram data using the QW-GPL-based SIDH systems with the three-stacked CLC or the AQWP. The reconstruction was performed separately for the full-color channel, red channel, green channel, and blue channel. In all channels, the QW-GPL-based SIDH system utilizing the three-stacked CLC showed much better evaluation values in image entropy, compared to the AQWP-based system, indicating effective noise reduction in the proposed approach for full-color GPL-based SIDH imaging.

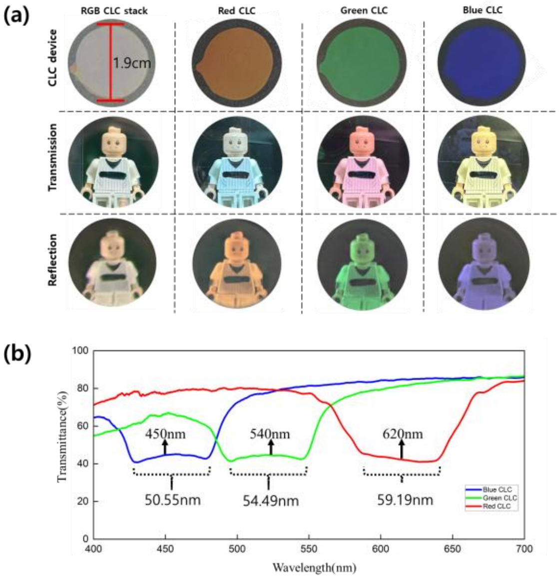

Fig 4. (a) The transmission and reflection characteristics of fabricated R/G/B CLC cells, observed for object images. (b) The spectral evaluations for the transmissive bandwidth characteristics of the R/G/B CLC cells.

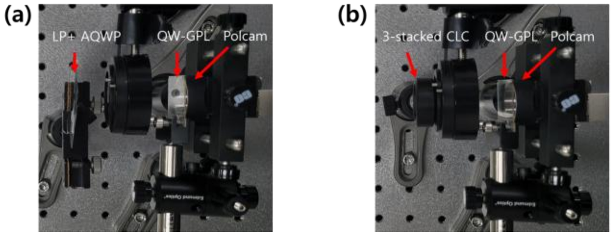

Fig 5. QW-GPL-based SIDH systems (a) at using a linear polarizer and AQWP as the conventional scheme and (b) at using three-stacked CLC module for a circular polarizer.

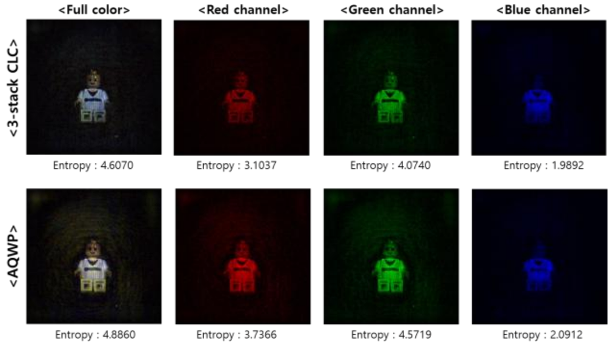

Fig 6. Full-color complex hologram results with QW-GPL-based SIDH, improved by using the three-stacked CLC module, where the results by using the AQWP are co-presented for comparison. The results, analyzed after the color-channel separations, are also presented, along with the image entropy analysis values.

3. Discussion & Conclusion

In this study, we present a SIDH system incorporating a QW-GPL-based architecture, an advancement that has not been explored until now. Conventional HW-GPL-based SIDH systems are prone to noise generation at a full color imaging, arising from three-wavefront interference at wavelengths outside the operational range of the HW-GPL [8]. In contrast, the QW-GPL-based SIDH system sustains two-wavefront interference across the entire visible spectrum under the condition of perfectly circularly polarized incident light, effectively mitigating noise associated with three-wavefront interference.

The QW-GPL-based SIDH system relies on the condition of dual sets of perfectly circularly polarized incident lights to achieve two-wavefront-based polarization interference for phase-encoded LP patterns via self-interference behavior. For ideal incident circular polarization state, the CLC stack module is also provided, replacing conventional retardation-based AQWP-based circular polarizer, where the proposed three-stacked CLC module exhibits ideal circular polarization states under the oblique light incidence for a wide field of view imaging as well as the full-visible spectrum. By incorporating the proposed both schemes of the three-stacked CLC circular polarizer and the QW-GPL-based SIDH imaging, complex holographic data were successfully acquired and reconstructed for full color ranges with the incoherent light source.

4. Impact of your research

This study represents the first application of applying the QW-GPL scheme within a self-interference-based SIDH system for ideal dual sets of wavefront modulations, establishing a foundation for overcoming typical noise issues in the full-color imaging with the SIDH system. By integrating the QW-GPL, we propose a fundamental solution to the retardation-based noise issue of three-wavefront interference in the visible spectrum, which was a challenging inherent problem in the conventional HW-GPL-based SIDH system. Furthermore, we have developed a three-stacked CLC circular polarization filter, specifically designed to optimize the integration of the QW-GPL-based in SIDH systems. This filter not only enhances the performance of the QW-GPL-based SIDH systems but also holds significant potential for application in other optical devices leveraging circular polarization for a wide range of spectral operations.

Through this research, we have proposed a new approach to noise reduction in the domain of holographic 3D information acquisition and presented a method to enhance the performance of devices operating on a circular polarization basis. Considering the unique advantages of the proposed approach over conventional holographic imaging technologies, these advancements are expected to be actively utilized in various application fields, such as full-color-based XR optical systems and bio-imaging optics.

5. Acknowledgements

This research was supported by the National Research Foundation (NRF) funded by the Korean government (MSIT) (No. RS-2024-00416272). This work was supported by Electronics and Telecommunications Research Institute (ETRI) grant funded by ICT R&D program of MSIT/IITP [2019-0-00001, Development of Holo-TV Core Technologies for Hologram Media Services]

6. References

1. Rosen J, Brooker G. Digital spatially incoherent Fresnel holography. Optics Letters.2007;32(8):912-914.
2. Jackin BJ, Narayanamurthy C. S., Yatagai T. Geometric phase shifting digital holography. Optics Letters. 2016;41(11):2648-2651.
3. Choi K, Yim J, Min SW. Achromatic phase shifting self-interference incoherent digital holography using linear polarizer and geometric phase lens. Optics Express. 2018;26(13):16212-16225.
4. Choi K, Joo KI, Lee TH, Kim HR, Yim J, Do H, Min SW. Compact self-interference incoherent digital holographic camera system with real-time operation. Optics Express. 2019;27(4):4818–4833.
5. Yamaguchi I, Zhang T. Phase-shifting digital holography. Optics letters. 1997;22(16):1268-1270.
6. E.Hajdo L, Eringen A. Theory of light reflection by cholesteric liquid crystals possessing atilted structure. Journal of the Optical Society of America. 1979;69(11):1509-1513.
7. Al-Shamasneh AR, Ibrahim RW. Image Denoising Based on Quantum Calculus of Local Fractional Entropy. Symmetry. 2023;15(2):396.
8. Choi K, Lee JW, Shin J, Hong K, Park J, Kim HR. Real-time noise-free inline self-interference incoherent digital holography with temporal geometric phase multiplexing. Photonics Research. 2023;11(6):906–916.